Magnetization distribution in CoS_2; is it a half metallic ferromagnet?

2005 J. Phys.: Condens. Matter 17 1583

(http://iopscience.iop.org/0953-8984/17/10/013)

INSTITUTE OF PHYSICS PUBLISHING JOURNAL OF PHYSICS: CONDENSED MATTER

J. Phys.: Condens. Matter **17** (2005) 1583–1592 doi:10.1088/0953-8984/17/10/013

Magnetization distribution in CoS_2; is it a half metallic ferromagnet?

P J Brown[1,2], K-U Neumann[2], A Simon[3], F Ueno[4] and K R A Ziebeck[2]

[1] Institut Laue Langevin, BP 156, 38042 Grenoble, France
[2] Department of Physics, Loughborough University, Loughborough LE11 3TU, UK
[3] Max Planck Institut für Festkörperforschung, 70569 Stuttgart, Germany
[4] Toshiba Corporation, Kawasaki, Japan

Received 12 November 2004, in final form 1 February 2005
Published 25 February 2005
Online at stacks.iop.org/JPhysCM/17/1583

Abstract

Polarized neutron diffraction has been used to determine the spatial distribution of the magnetization in CoS_2 and its temperature dependence. Although the previously reported ground state moment 0.84 μ_B is non-integral, the compound has sometimes been classified as a half metallic ferromagnet. The present results show that the ferromagnetic phase cannot have half metallic properties. The magnetization distribution around the Co^{2+} ions in the ferromagnetic phase at 1.8 K is nearly spherical, indicating that, contrary to electronic structure calculations, electrons both of e_g and t_{2g} character contribute to the observed magnetic moment. The orbital contribution to the moment is found to be small, a factor of two less than that determined from magnetic circular dichroism measurements. A small moment, approximately 2% of that on the cobalt ions, resides on the sulfur atoms at 1.8 K. The magnetization distribution induced in the paramagnetic phase by a field of 9.6 T at 150 K is significantly different from that in the ferromagnetic state and has the asphericity characteristic of e_g electrons. On heating to 300 K and then to 400 K the t_{2g} character of the magnetization increases continuously and becomes predominant above the anomaly in the susceptibility at 350 K.

The authors PJB, KUN, FU and KRAZ would like to dedicate this paper to Arndt Simon on the occasion of his 65th Birthday.

1. Introduction

Although the transition metal disulfides MS_2(M = Fe, Co, Ni) form an isomorphous series with the pyrite structure they exhibit a wide variety of physical properties [1]. A qualitative description of their disparate magnetic and electrical properties has been given in terms of successive filling of the e_g orbitals of the transition metal ions [2, 3]. In the pyrite structure the strong octahedral field splits the 3d bands of the metal ions into t_{2g} and e_g sub-bands with the t_{2g} band having sufficiently lower energy that the metal ions are in low spin states with

configurations $t_{2g}^6 e_g^0$, $t_{2g}^6 e_g^1$ and $t_{2g}^6 e_g^2$, for Fe, Co and Ni respectively. FeS_2 with fully occupied t_{2g} and empty e_g bands is a semiconductor with an energy gap of ≈0.8 eV whereas CoS_2 is a ferromagnetic metal with $T_C \approx 120$ K. Due to the large on site Coulomb correlation NiS_2 is an antiferromagnetic insulator, $T_N \approx 40$ K, with a half filled e_g band.

Amongst the members of the pyrite series CoS_2 is of particular interest since according to the above model the open band contains electrons with a single spin state. It should therefore exhibit half metallic conduction which might be exploited in spin dependent electronic devices. The simple model is however not adequate to explain all the relevant properties. In the ferromagnetic ground state the saturation moment is 0.84 μ_B/Co atom which is close to, but not equal to, the value expected for $S = \frac{1}{2}$ [4]. Magnetic circular dichroism measurements have been interpreted as showing that the Co atoms have a significant orbital magnetic moment $L_z/S_z = 0.18$ [5] and 0.14 [6]. Such a large orbital moment is unexpected for Co in the low spin state with a large crystal field splitting ≈2.5 eV. If this interpretation were correct, the spin moment would be even less than 0.84 μ_B ($\mu_{Tot} = \langle L_z \rangle + 2\langle S_z \rangle$). The thermal variation of the uniform reciprocal susceptibility is reported to show an anomaly around 350 K, a feature which has been interpreted as arising from spin fluctuations [7]. Neutron scattering experiments below T_C [8–10] show a clear broadening of the spin wave excitations as they enter the Stoner continuum and in the paramagnetic state the response is diffusive and can be described using dynamical scaling. On the other hand it has been argued, on the basis of photo-emission spectroscopy, that the electronic structure in the paramagnetic phase should be described by a localized model [11]. It has even been suggested that CoS_2 is a good candidate to exhibit orbital ordering [12], but no evidence for the consequent loss of symmetry has yet been observed. Polarized neutron diffraction measurements show that in the ordered phase the moment is predominantly localized on the cobalt atoms [13, 14].

Although the variation in the physical properties of compounds in the MS_2 series may be qualitatively understood in terms of a sequential filling of the e_g manifold the details depend upon the changing influence of electron correlation. In order to resolve some of the conflicting results and to determine whether CoS_2 is in fact a half metallic ferromagnet a new polarized neutron diffraction investigation of the magnetization distribution has been carried out as a function of temperature. The results of this investigation are presented here.

2. Structural and magnetic properties

CoS_2 crystallizes with the cubic pyrite structure, illustrated in figure 1. The cobalt ions are octahedrally coordinated by sulfur which themselves form S_2^{2-} dimers [15]. Each sulfur (e.g. A in figure 1) is shared by three different octahedra and a single dimer. The structural details are given in table 1. CoS_2 orders ferromagnetically below 120 K, with an ordered moment of 0.84 μ_B per cobalt atom in the ground state [4]. At 5 K the magnetization reaches saturation in a field of only ≈0.2 T showing that the magnetic anisotropy is small. The thermal variation of the spontaneous magnetization below about $T_C/3$ has a $T^{3/2}$ dependence as expected for spin waves in an isotropic Heisenberg ferromagnet [4]. The nearest neighbour exchange constant derived from this analysis is $J_{nn} \approx 3$ meV. Subsequent inelastic neutron scattering experiments [8–10] at 80 K give a spin wave stiffness constant $D = 107$ meV Å^{-2}. Assuming $S = \frac{1}{2}$ this gives $J_{nn} = Da^{-2} = 3.5$ meV. Isotropic spin waves with a slightly larger spin wave stiffness constant $D = 132$ meV Å^{-2} have been measured in $CoS_{1.9}Se_{0.1}$ [16]. In this latter investigation the renormalization of the spin wave stiffness constant up to 0.9 T_C was found to be small and consistent with a Heisenberg two-magnon process. In stoichiometric CoS_2 well defined spin waves were only found for wavevectors below ≈0.27 Å^{-1} corresponding to energies below ≈8 meV. Above this energy, the spin wave excitations broaden consistent with their entry into a

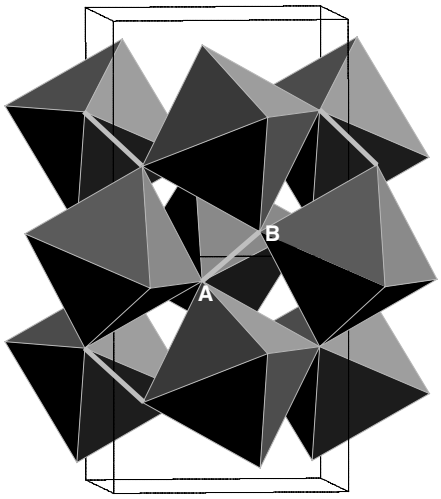

Figure 1. Schematic representation of the pyrite structure of CoS_2 illustrating the linkage of the CoS_6 octahedra. The S–S dimers are marked by lines of the type shown by A–B.

Table 1. Structural parameters for CoS_2 at 150, 293 and 400 K.

Space group $Pa\bar{3}$		$a = 5.539$ Å at 300 K		
4Co in 4a (0,0,0)			8S in 8c (x, x, x)	
	T (K)	Co μ (μ_B)	Co ITF (Å^2)	S x	S ITF (Å^2)
	20	0.882(14)	0.144(8)	0.389 88(4)	0.168(7)
Small crystal	150		0.217(8)	0.389 88(4)	0.231(6)
	400		0.502(15)	0.389 98(6)	0.512(13)
Large crystal	293		0.329(5)	0.389 89(2)	0.328(4)

Stoner continuum, suggesting itinerant behaviour. On the other hand the uniform susceptibility is strongly temperature dependent above T_C, indicating that the exchange splitting persists. The inverse susceptibility has a Curie–Weiss behaviour but with an apparent change of slope at approximately 350 K [4, 17]. The higher temperature regime leads to a paramagnetic Curie temperature of 220 K and an effective moment of 1.77 μ_B which is close to the value of 1.732 μ_B expected for $S = \frac{1}{2}$ and $g = 2$. The paramagnetic Curie temperature calculated using the Heisenberg model and the measured exchange constant ($kT_p = \frac{2}{3}S(S+1)N_{nn}J_{nn}$) is $\approx$231 K in close agreement. The behaviour of the inverse susceptibility below 350 K leads to a paramagnetic Curie temperature of 125 K and effective moment of 2.56 μ_B giving $S = 0.88$. This anomaly in the uniform susceptibility has been attributed to spin fluctuations the amplitudes of which saturate above 350 K [7]. Neutron scattering measurements show that the paramagnetic response above T_C is centred at zero energy transfer and can be described by a double Lorentzian in q and ω [10].

A polarized neutron study of the magnetization distribution in the ferromagnetic phase of CoS_2 at 93 K has already been undertaken [13, 14]. It led to the conclusion that 69% of the magnetic electrons were in e_g orbitals and that a significant moment amounting to about 4% of the cobalt moment was transferred to sulfur 3p electrons. However, these results must be treated with caution because the authors interpreted their data assuming that the Co^{2+} ions had full cubic point group symmetry rather than the $\bar{3}$ symmetry characteristic of the metal sites in the pyrite structure. Furthermore, they attributed all the scattering in the mixed odd and even index reflections to sulfur, neglecting the contribution from aspherical magnetization associated with cobalt.

There have been various attempts to clarify the magnetic behaviour of CoS_2 using band structure calculations. Zhao [18] using the LCAO approximation found that CoS_2 is nearly half metallic in the sense that there are few electrons in the minority-spin band. More recently, Hobb and Hafner [19] studied the ground state cohesive properties of CoS_2 and obtained similar results using the projected APW method. In fact recent experimental reflectivity data have been interpreted consistently under the assumption of half metallic behaviour [20]. In contrast with the above results further LMTO calculations [21] lead to a fully metallic ground state with a partially filled minority-spin e_g band.

3. Experimental details

3.1. Single-crystal samples

Polycrystalline CoS_2 [22] was made by slowly heating a stoichiometric mixture of cobalt powder (Johnson Matthey, 99.998%) and sulfur from an ingot (Ventron, 99.9995%) to 1073 K in a closed silica tube and quenching it into a water bath after 7 days. Single crystals were grown from the polycrystalline material by chemical transport [23]. 5 g of CoS_2 were placed in a silica tube (30 mm diameter, 100 mm long) containing saturated Cl_2 vapour over liquid chlorine at 216 K. After 16 days in a temperature gradient of 1166–1155 K a few crystals with sizes around 5 mm^3 had grown. They were identified as CoS_2 by x-ray single-crystal diffraction measurements.

The single crystals obtained were irregularly developed cube octahedra with face indices {111} and {100}. Two well formed crystals of different sizes were chosen for the experiments; the smaller had linear dimensions $\approx$2 mm^3 and the larger $\approx$4 mm^3. The former was used for the measurements in the ferromagnetic and low temperature paramagnetic phases in order to minimize the effects of extinction and the latter for the measurements at 300 and 400 K where the magnetic scattering is expected to be an order of magnitude smaller.

3.2. Unpolarized neutron diffraction

In order to determine the structural parameters and the extent to which extinction was present in the crystals, sets of integrated intensities were measured with unpolarized neutrons using the D9 single-crystal diffractometer at the ILL. The crystals were mounted with a $[1\bar{1}0]$ axis approximately parallel to the ϕ axis of the diffractometer.

The integrated intensities of approximately 400 reflections from the small crystal with $\sin\theta/\lambda < 1.0$ $Å^{-1}$ were measured at three temperatures: 20, 150 and 400 K. At this time the hot source at the ILL was not functioning and therefore a single neutron wavelength of 0.84 Å was used. The three temperatures chosen correspond to the ferromagnetic phase and to the two different paramagnetic regimes revealed by susceptibility measurements. For the two lower temperatures the sample was mounted in a double-stage Displex refrigerator and for the 400 K set it was remounted in a four-circle resistance furnace. The integrated intensities of equivalent reflections measured at the same temperatures were found to be in good agreement. After averaging equivalent reflections together a set of approximately 200 independent structure factors was obtained at each temperature. These were used in a least squares refinement to determine a scale factor, the sulfur x parameter, two isotropic temperature factors and a single extinction parameter: the mosaic spread of the Becker–Coppens extinction model for a type I crystal [24]. For the data set obtained at 20 K the cobalt magnetic moment was also refined. The structure parameters obtained are reported in table 1. Although the mosaic spread was found to be rather small the absolute reflectivities are also small and the maximum extinction factor was 1.35, which corresponds to a diminution in intensity of only 35%.

The integrated intensities from the larger crystal were measured in a subsequent experiment when the new ILL hot source was operational. The accessible reflections in one half of reciprocal space were measured at ambient temperature and three wavelengths, namely 0.836, 0.51 and 0.352 Å. The intensities of equivalent reflections measured at each wavelength were averaged so as to give a set of intensities for independent reflections at each wavelength. The results of a least squares refinement, in which all three data sets were included, are given in the bottom line of table 1. The maximum extinction factor was 1.94 in intensity for the 440 reflection measured at 0.84 Å. Support for the validity of the extinction model is provided by the good accordance shown in table 1 of the structure parameters, in particular the temperature factors, with those determined using the small crystal at 150 and 400 K. It can be seen from table 1 that the moment per cobalt atom at 20 K is in good agreement with that reported on the basis of magnetization measurements. Furthermore, the sulfur positional parameter x does not vary significantly over the temperature range covered in the experiment.

3.3. Polarized neutron diffraction

The polarized neutron diffractometer D3 at the ILL was used to determine the flipping ratios in two series of experiments. In the first, the smaller crystal was mounted with a $[1\bar{1}0]$ axis approximately vertical in the variable temperature insert of a 10 T superconducting magnet. The flipping ratio of all accessible reflections with $\sin\theta/\lambda < 0.6$ Å^{-1} were measured in an applied field of 9.6 T, first in the ferromagnetic phase at 1.8 K and then in the paramagnetic phase at 150 K. The reflections for CoS_2 can be divided into two types: those with h, k and l all even or all odd (fundamental), and mixed index reflections. Magnetization distributed around the Co atoms which has full cubic symmetry will only contribute to the fundamental reflections. Any magnetic contribution to the mixed reflections is due either to non-cubic components of the Co magnetization or to the magnetic moment associated with sulfur. The flipping ratios of these mixed reflections were found to be close to unity. For the second set of experiments at 400 K the larger crystal was mounted also with a $[1\bar{1}0]$ axis approximately vertical, but this time in a special high temperature insert for the 10 T superconducting magnet. Measurements of the mixed index reflections were restricted to a small group which had been found to have significant magnetic content in the measurements made at 150 K. A limited set of data was also collected at 300 K.

Magnetic structure factors were calculated from the measured flipping ratios using the structural and extinction parameters obtained from the integrated intensity measurements. The values obtained for equivalent reflections were averaged together, and their standard deviations estimated from the differences of individual measurements from their mean. The final data sets at 1.8, 150, 300 and 400 K contained respectively 36, 33, 25 and 27 independent reflections.

4. Analysis of the results

Fourier analysis of the data obtained at 1.8 K did not immediately reveal any asymmetry characteristic of e_g electrons, or any significant magnetization around the sulfur atoms. In order to reduce effects due to the sparsity and noisiness of the data, a maximum entropy algorithm was used to construct a model free representation of the distribution of magnetization in real space [25]. 110 sections through the origin of the distribution obtained at 1.8 and 150 K are shown in figures 2(a) and (b) where they are compared with the distribution calculated for Co^{2+} in the $t_{2g}{}^6e_g{}^1$ configuration (c). The map obtained for the data measured at 1.8 K (figure 2(a)) shows a nearly spherical distribution of magnetization around cobalt, whereas that for the data measured at 150 K (figure 2(b)) shows some evidence of the asymmetry characteristic

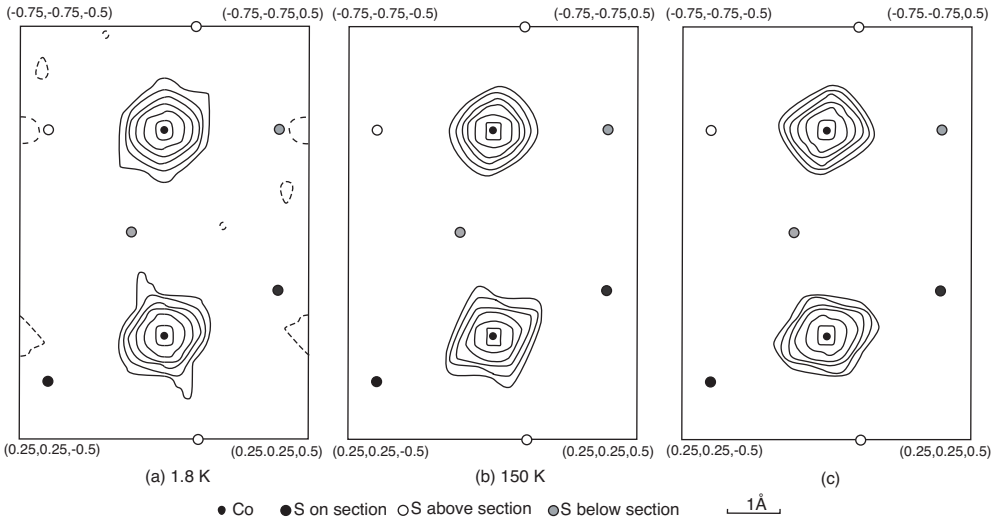

Figure 2. Sections perpendicular to $[1\bar{1}0]$ through the origin of the maximum entropy reconstruction of the magnetization distribution in CoS_2 (a) at 1.8 K and (b) at 150 K in 9.6 T. (c) The distribution obtained with the same reflections given the same weights as for (a), but using structure factors calculated for a Co^{2+} ion in the $t_{2g}{}^6e_g{}^1$ configuration. Adjacent contours differ by a factor of two; the highest in (a) corresponds to 2 μ_B Å^{-3}; (b) and (c) have been scaled to the same maximum value. The peaks around 000 and $\frac{\bar{1}}{2}\frac{\bar{1}}{2}0$ show differently orientated sections through the cobalt magnetization distribution.

of e_g electrons (figure 2(c)). Neither of the experimental maps shows any significant magnetization around the sulfur atoms.

A more quantitative analysis of the data was made by modelling the density with the sum of multipole functions, having appropriate radial densities, centred on the atomic sites. For the pyrite structure the point group symmetry of the metal site is $\bar{3}$ and the multipoles permitted by symmetry (up to order 4) are Y_0^0, Y_2^0, Y_4^0, Y_4^3 and Y_4^{-3}. This trigonal perturbation of the octahedral crystal field maintains the twofold degeneracy of the cubic e_g orbitals but splits the t_{2g} set into a single orbital transforming as A_1 and a second twofold degenerate set with E symmetry. When written in terms of right handed orthogonal axes defined with z parallel to the triad and the x–z plane containing one of the Co–S bonds the e_g and t_{2g} functions assume the form

$$\begin{aligned} e_g \quad &\rightarrow \quad e_1 = \sqrt{\tfrac{1}{3}}(Y_2^2 + \sqrt{2}Y_2^{-1}) \quad \text{and} \quad e_2 = \sqrt{\tfrac{1}{3}}(Y_2^{-2} - \sqrt{2}Y_2^1) \\ t_{2g} \quad &\rightarrow \quad a_1 = Y_2^0 \\ &\qquad\quad t_1 = \sqrt{\tfrac{1}{3}}(\sqrt{2}Y_2^2 - Y_2^{-1}) \quad \text{and} \quad t_2 = \sqrt{\tfrac{1}{3}}(\sqrt{2}Y_2^{-2} + Y_2^1). \end{aligned} \tag{1}$$

The a_1 function transforms as the A_1 representation of the point group $\bar{3}$ and the e and t functions subscripted 1 and 2 belong respectively to the E_1 and E_2 representations. The angular parts of the corresponding probability densities are given by

$$\begin{array}{llll} Y_0^0 & +\frac{\sqrt{20}}{7}Y_2^0 \quad +\frac{6}{7}Y_4^0 & & \text{for } a_1 \\ Y_0^0 & \quad -\frac{1}{3}Y_4^0 & +\sqrt{\frac{10}{63}}Y43+ & \text{for } e_1 \text{ and } e_2 \\ Y_0^0 & -\frac{\sqrt{5}}{7}Y_2^0 \quad -\frac{2}{21}Y_4^0 & -\sqrt{\frac{10}{63}}Y43+ & \text{for } t_1 \text{ and } t_2 \end{array} \tag{2}$$

Table 2. Goodness of fit parameters χ^2 for different models of the magnetization distribution in CoS_2 at 2, 150, 300 and 400 K. (Note: $\chi^2 = (N_{obs} - N_{pars})^{-1} \sum[(F_{obs} - F_{calc})/\sigma(F_{obs})]^2$.)

Model	2 K[a]	150 K	300 K	400 K
Spherical Co	9.2	6.2	2.4	6.9
Spherical Co with orbital expansion	9.3	5.2	2.4	5.5
Spherical Co with S 3p	8.8	5.6	2.0	7.1
Spherical Co with orbital expansion and S 3p	8.9	5.4	1.9	5.7
Multipolar Co	7.8	4.4	2.8	2.6
Multipolar Co with orbital expansion	7.9	3.8	2.8	2.6
Multipolar Co with orbital expansion and S 3p	7.3	4.0	2.3	2.6

[a] The higher final χ^2 values reflect the greater statistical accuracy of the measurements for this data set.

where $Y43+$ represents the real combination of spherical harmonic functions $\sqrt{\frac{1}{2}}(Y_4^3 - Y_4^{-3})$. Note that for this choice of axes the combination $Y43- = -\frac{\mathrm{i}}{\sqrt{2}}(Y_2^3 + Y_4^{-3})$ does not occur although it is allowed by symmetry. The orientation of the x axis is not however imposed by symmetry; a rotation by an angle ϕ about the z axis leads to the appearance of the $Y43-$ combination of spherical harmonics in the density. The amplitudes of the $Y43+$ and $Y43-$ combinations in the densities corresponding to rotated e and t functions are given by $\pm\sqrt{\frac{10}{63}}\cos 3\phi$ and $\pm\sqrt{\frac{10}{63}}\sin 3\phi$ respectively. In terms of the original e and t functions (equation (1)) such rotation corresponds to coherent mixing of e_1 with t_1 and e_2 with t_2 to give functions having the forms

$$et_1 = \cos\frac{3\phi}{2}e_1 + \mathrm{i}\sin\frac{3\phi}{2}t_1 \qquad \text{and} \qquad te_1 = \sin\frac{3\phi}{2}e_1 - \mathrm{i}\cos\frac{3\phi}{2}t_1. \quad (3)$$

The magnetic structure factors were fitted by a least squares procedure to a model in which the cobalt magnetization has the radial distribution of the Co^{2+} free ion and an angular distribution corresponding to some combination of the functions given above. The magnetic structure factor for this model can be written as

$$F(\mathbf{k}) = \frac{4}{n_g}\sum_i \sum_{L,M} \left(\langle j_L(k)\rangle a_{LM} Y_{LM}(\tilde{\mathbf{R}}_i\hat{\mathbf{k}}) \exp(\mathrm{i}\mathbf{k}\cdot\hat{\mathbf{t}}_i) \right) \quad (4)$$

where the sum in i is over all n_g operators $\{\tilde{\mathbf{R}}_i : \hat{\mathbf{t}}_i\}$ in the space group and that over L, M is restricted to the pairs of L and M appearing in equation (2) with the addition of the combination $Y43-$. The $\langle j_L(k)\rangle$ are the radial form factors for the Co^{2+} free ion. This simple model was extended by allowing some flexibility in the radial form factor for $L = 0$ which was expressed as $(a_{00}\langle j_0\rangle + j_2\langle j_2\rangle)$ where a_{00} and j_2 are parameters of the refinement. The possibility of magnetic moment associated with the sulfur atoms was also investigated by adding a term $pF_s(\mathbf{k})f_s(k)$ to the magnetic structure factor. $F_s(\mathbf{k})$ is the geometric structure factor of the sulfur atoms, $f_s(k)$ a spherical form factor calculated from the sulfur 3p electron distribution [26] and p a refinable parameter. The effects of varying the number of parameters included in the refinement at all four temperatures are shown in table 2. Except for the data at 150 K the fit is not significantly improved by including the j_2 term, showing that the radial distribution of the magnetization is essentially the same as that of the free Co^{2+} ion. For the data at 300 K there is no significant departure from spherical symmetry although the fit at this temperature and at 1.8 K is improved by including a moment on sulfur. The values of the parameters derived for the model giving the best fit to the data at 1.8, 150, 300 and 400 K are given in table 3.

Table 3. Values of the parameters obtained for the models giving the best fit to the magnetization distribution in CoS_2 at 2, 150, 300 and 400 K.

Parameter	2 K	150 K	300 K	400 K
Co a_{00}	0.92(4)	0.354(7)	0.0647(6)	0.0393(14)
Co a_{20}	−0.010(17)	−0.015(17)		−0.003(5)
Co a_{40}	−0.13(18)	−0.07(5)		0.004(18)
Co a_{43+}	−0.02(9)	0.18(9)		−0.007(17)
Co a_{43-}	0.11(9)	0.08(5)		0.022(10)
Co j_2	−0.06(7)	0.05(2)	−0.006(4)	−0.04(4)
S p	0.016(9)		0.0021(8)	
χ^2	8.9	4.0	1.9	2.6
R factor (%)	15	12	15	18

5. Discussion

From table 1 it may be seen that the sulfur positional parameter does not change with temperature, over the range 20–400 K covered in the investigation. Furthermore, x-ray powder diffraction measurements show that the lattice parameter increases smoothly up to 300 K, with no apparent anomaly at T_C. Electronic structure calculations [19] also predict a relatively weak magneto-volume effect. However, these same calculations suggest that there should be a reduction in the length of the bond between S–S pairs with the onset of magnetic order. The structure refinements reported in section 4 show that no such reduction in the separation of the S–S dimer occurs. The thermal variation of the susceptibility and the observed paramagnetic scattering both indicate that the exchange splitting does not collapse at the Curie temperature. All these results suggest that the magnitude of the local moment and hence the atomic volume is essentially fixed. On the other hand the change in slope of the inverse susceptibility versus temperature curve indicates a change in the effective moment at around 300 K. Whereas the effective paramagnetic moment above 350 K is close to that expected for $S = \frac{1}{2}$, at lower temperatures it is significantly higher. The present experiments show that the spatial distribution of the electrons giving rise to the magnetization also changes with temperature.

Band structure calculations made using different techniques all predict that the Fermi level falls in the e_g sub-band and that it is electrons in this sub-band which give rise to the magnetic and thermodynamic properties. A summary of results derived from different band structure calculations is given in table 4. The polarized neutron results given in table 3 can be used to deduce a similar set of properties for the wavefunctions of the electrons which give rise to the magnetization at the temperatures of the experiment. The occupancies of the a_1, et and te orbitals and the value of the angle ϕ which best fit the multipole parameters have been calculated and are given in table 5. It can be seen from the table that the fractional occupancies at 1.8 and 300 K are very similar, corresponding to a nearly spherical distribution of magnetization around cobalt, whilst only at 150 K do the occupancies approach those expected from the simple low spin ionic model. The analysis shows that the orbital moment, measured by the parameter j_2 is not significant except at 150 K where it contributes about 15% of the total moment, less than half of that proposed on the basis of magnetic circular dichroism measurements.

A qualitative explanation of the results can be given in terms of a band structure leading to a density of states (DOS) similar to that given by Kwon *et al* [28]. It must however be postulated that the exchange splitting in the ferromagnetic state is enough to cause a partial overlap of the minority spin a_1 and te bands with the majority spin et band; as shown in the schematic DOS of figure 3(a). The magnetic moment in the ordered state is then due to holes in the top of the minority spin a_1 and te bands and electrons in the bottom of the et band. It is also expected that

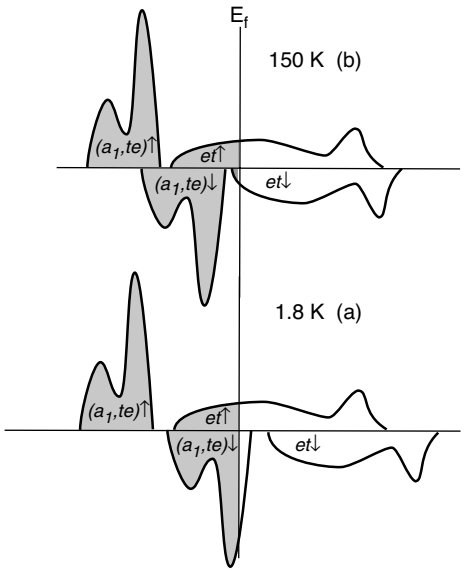

Figure 3. Schematic plot of the DOS near the Fermi energy E_f, needed to account for the observed magnetization distribution in CoS_2 (a) in the ferromagnetic phase at 1.8 K and (b) at 150 K just above T_C.

Table 4. Magnetic moments for Co and S obtained in various band structure calculations for CoS_2 compared with the values obtained at 1.8 K in the present experiment.

	Cobalt		Sulfur		
μ_S (μ_B)	μ_L (μ_B)	Total (μ_B)	μ (μ_B)	Method	Reference
0.65	0.046	0.70	0.020	FPLMTO	[27]
		0.76		LAPW	[19]
0.73		0.73	0.032		[21]
0.80	0.060	0.86	0.04	LSDA	[28]
0.98(8)	−0.06(7)	0.92(4)	0.016(9)	Experiment	

Table 5. Properties of the Co 3d and S 3p wavefunctions contributing to the magnetization distribution at 1.8, 150, 300 and 400 K

Temperature	1.8 K	150 K	300 K	400 K
Co moment (μ_B)	0.92(4)	0.354(7)	0.0647(6)	0.0393(14)
$a1$ occupancy (%)	18(7)	0(10)	20(5)	25(8)
et occupancy (%)	40(19)	97(26)	40(10)	0(24)
te occupancy (%)	42(14)	3(19)	40(16)	75(13)
e:t mixing angle ϕ (deg)	−32(15)	−8(6)		−36(13)
e:t mixing ratio (%e in et)	45(35)	95(7)		37(33)
Radial expansion j_2/a_{00} (%)	−6(7)	15(7)	−11(9)	−10(9)
μ_S/μ_{Co} (%)	2(1)	0(2)	3(2)	0(4)

it will be at the top of the te band and at the bottom of the et band that the e_g, t_{2g} mixing will be strongest and this can account for the large value of the mixing angle ϕ observed at 1.8 K. At T_C it is postulated that there is a partial collapse of the exchange splitting as illustrated in figure 3(b). The DOS then closely resembles that given by band structure calculations for the ordered state. The ordered paramagnetic magnetization is due just to electrons in the majority spin et band and accordingly has nearly pure e_g character. Indeed, the asphericity observed in the early polarized neutron experiment at 93 K [13] suggests that the exchange splitting decreases with increasing temperature even below T_C. To account for the higher temperature

behaviour the top of the minority spin *te* band must lie sufficiently close to the Fermi energy for thermal excitation to create holes in it which can contribute to the magnetization at 300 K. These must add enough t_{2g} character to give nearly spherical symmetry. This *te* component is further excited at 400 K.

The data obtained at 1.8 K suggest that a magnetic moment of approximately 2% of that on cobalt is associated with sulfur. This is of the same order of magnitude as, though somewhat smaller than, that deduced from the band structure calculations and shown in table 4. The precision obtained at higher temperatures is not sufficient to say with certainty whether the same degree of polarization of sulfur is present in the paramagnetic phase.

The magnetization distribution observed in the present experiments on CoS_2 shows that, in the ferromagnetic phase, bands of both e_g and t_{2g} character contain unpaired electrons. A similar result was obtained for the ferromagnetic Heusler alloy Co_2MnSi which has also been proposed as a half metallic system [29]. Consequently, neither of these systems can have a band structure which would give the ideal half metallic ferromagnetism required for spin injection devices in spintronic applications. Interestingly, the distribution of magnetization aligned by a magnetic field at 150 K, just above T_C, is closely similar to that which is predicted from band structure calculations for the ferromagnetic phase and has nearly pure e_g character. On further heating, orbitals with t_{2g} character contribute more and more to the magnetization and above the susceptibility anomaly at 350 K they become predominant.

References

[1] Wilson J A and Yoffe A D 1969 *Adv. Phys.* **18** 193
[2] Bullet D W 1982 *J. Phys. C: Solid State Phys.* **15** 6163
[3] Ogawa S 1979 *J. Appl. Phys.* **50** 2308
[4] Adachi K, Sato K and Takeda M 1969 *J. Phys. Soc. Japan* **26** 631
[5] Muro T, Shishidou T, Oda F, Fukawa T, Yamada H, Kimura A, Imada S, Suga S, Park S Y, Miyahara T and Sato K 1996 *Phys. Rev.* B **53** 7055
[6] Miyauchi H, Koide T, Shidara T, Nakajima N, Kawabe H, Yamaguchi K, Fujimori A, Fukutani H, Iio K and Miyadai T 1996 *J. Electron Spectrosc. Relat. Phenom.* **78** 255
[7] Moriya T and Usami K 1980 *Solid State Commun.* **34** 95
[8] Hiraka H, Matsuura M, Yamada K and Endoh Y 1997 *Physica* B **237/238** 478
[9] Hiraka H, Endoh Y and Yamada K 1998 *J. Magn. Magn. Mater.* **177–181** 1349
[10] Hiraka H, Endoh Y and Yamada K 1997 *J. Phys. Soc. Japan* **66** 818
[11] Fujimori A, Mamiya K, Mizokawa T, Miyadai T, Sekiguchi T, Takahashi H, Môri N and Suga S 1996 *Phys. Rev.* B **54** 16329
[12] Cyrot M and Lyon-Caen C 1975 *J. Physique* **36** 253
[13] Ohsawa A, Yamaguchi Y, Watanabe H and Itoh H 1976 *J. Phys. Soc. Japan* **40** 986
[14] Ohsawa A, Yamaguchi Y, Watanabe H and Itoh H 1976 *J. Phys. Soc. Japan* **40** 992
[15] Wyckoff R W G 1965 *Crystal Structure* vol 1 (New York: Interscience)
[16] Sato T J, Lynn J W, Hor Y S and Cheong S-W 2003 *Phys. Rev.* B **68** 214411
[17] Jarrett H S, Cloud W H, Bouchard R J, Butler S R, Frederick C G and Gillson J L 1968 *Phys. Rev. Lett.* **21** 617
[18] Zhao G L, Callaway J and Hayashibara M 1993 *Phys. Rev.* B **48** 15781
[19] Hobbs D and Hafner J 1999 *J. Phys.: Condens. Matter* **11** 8197
[20] Yamamoto R, Machida A, Morimoto Y and Nakamura A 1999 *Phys. Rev.* B **59** R7793
[21] Yamada H, Terao K and Aoki M 1998 *J. Magn. Magn. Mater.* **177–181** 607
[22] Andresen A F, Furuseth S and Kjekshus A 1967 *Acta Chem. Scand.* **21** 3
[23] Schäfer H 1964 *Chemical Transport Reactions* (New York: Academic)
[24] Becker P J and Coppens P 1974 *Acta Crystallogr.* A **30** 129
[25] Papoular R J and Gillon B 1990 *Europhys. Lett.* **13** 429
[26] Clementi E and Roetti C 1974 *At. Data Nucl. Data Tables* **14** 177
[27] Ahuja R, Eriksson O and Johansson B 1998 *Phil. Mag.* **78** 475
[28] Kwon S K, Youn S J and Min B I 2000 *Phys. Rev.* B **62** 357
[29] Brown P J, Neumann K-U and Ziebeck K R A 2000 *J. Phys.: Condens. Matter* **12** 1827